의학박사 학위논문

자기장 내 영상 왜곡을 최소화하기 위한 새로운 재질의 뇌동맥류 결찰술용 클립 개발연구

2017년 7월

서울대학교 대학원
의학과 신경외과학 전공
손 영 제

Abstract

Development of cerebral aneurysm clips to minimize susceptibility artifact by magnetic resonance imaging

Young-Je Son
College of Medicine (Neurosurgery)
The Graduate School
Seoul National University

OBJECTIVE: Surgical clipping is a major treatment modality in treating cerebral aneurysms. However, in magnetic resonance (MR) imaging, susceptibility artifact due to metal clips impedes postoperative assessments of clipped aneurysms, parent arteries, and adjacent parenchyma. Our goal was to develop an MR-compatible aneurysm clip.

METHODS: To reconcile mechanical/biologic properties with MR demands, we fabricated a prototypic clip (ZC: straight, 9-mm long), made of zirconia (body) and polyurethane (spring). Mechanical properties, closing forces, open-blade width, and artifact volumes (*in vitro and in vivo*) by 3T MR imaging of ZC and currently available metal clips (Yasargil [YC: curved, 8.3-mm long] and Sugita [SC: straight, 10-mm long]) were compared, using a canine venous pouch aneurysm model for *in vivo* study.

RESULTS: Respective closing force (N) values, measured at 1-mm and 8-mm distances from blade tip, were 2.09 and 3.77 in YC, 1.85 and

3.04 in SC, and 2.05 and 4.60 in ZC. Maximum open-blade widths (mm) were 6.8, 9.0, and 3.0 in YC, SC, and ZC, respectively. *In vitro* artifact volumes of YC and ZC were 26.0- and 1.9-fold greater than corresponding actual volumes. *In vivo* artifact volumes of YC, SC, and ZC were 21.4-, 29.4-, and 2.6-fold greater than actual volumes.

CONCLUSION: Compared with two clips in current use, our prototypic clip showed the least susceptibility artifact, with satisfactory closing forces. However, its narrow open-blade width was a weak point. Further experimentation is needed for design refinements and durability testing before human application is feasible.

.....

keywords: MR compatibility, cerebral aneurysms, clips, zirconia, susceptibility artifact

Student Number : 2004-30621

Contents

Introduction

Coil embolization and surgical clipping are mainstay modalities in treating cerebral aneurysms.[1] Postoperative follow-up imaging is critical in assessing treated aneurysms for future management plans. Typically, computed tomographic angiography (CTA), magnetic resonance angiography (MRA), and digital subtraction angiography (DSA) are utilized for this purpose. However, the adequacy of these imaging tools in delineating treated aneurysms does vary according to therapeutic approach. Clipped aneurysms are better visualized via CTA and DSA than by MR, given the susceptibility artifact of metal clips in MR images.[2,3,4] On the other hand, platinum-coil embolization is better assessed through MR and DSA than by CTA, where coils display beam hardening artifact.[5] Although DSA remains the best option overall, it is invasive and carries a remote risk of profound complications. Recently, attention has also been drawn to the radiation exposure inherent in both DSA and CTA, and the use of contrast media for MRA, CTA, and DSA is problematic in patients who are hypersensitive to contrast or suffer kidney dysfunction. Without use of contrast, MRA is still considered useful in monitoring coiled aneurysms, even stent-assisted coiling. Neither radiation nor contrast use are issues with MR, but its high cost and restriction to surgical clipping are limitations.[6,7]

Recently, complex therapeutic scenarios are increasing, such as multiple variably treated aneurysms (some clipped, coil embolization of others) in the same patient and remnant or recurrent aneurysms after one mode of treatment that are retreated by alternate approach. In such situations, the only viable means of follow-up imaging is DSA.

Therefore, we sought to develop a new aneurysm clip demonstrating MR compatibility and mechanical properties comparable to conventional metal clips.

Materials and Methods

Preparation of candidate raw materials for use in novel clip

Commercially available 3 mol% Y_2O_3-stabilized ZrO_2 (TZ-3Y-E grade, Tosoh Corp, Tokyo, Japan) and TiO_2 (titanium [IV] oxide, anatase >98%; Kanto Chemical Corp, Tokyo, Japan) were used as raw materials for clip blades. Cylindrical dies (11-mm diameter) filled with each powder compound were pressed (2000 psi, 10 min), forming 2-mm thick disk-shaped pellets. To achieve higher packing density, the pellets were also subjected to cold isostatic pressing (200 MPa). The green compacts were then carefully loaded into an Al_2O_3 crucible and sintered in a convection furnace (atmospheric pressure, 1450 ℃, 4 hours), heated at 5 ℃/min.

Polyurethane (Aidmer 78-185; Aidmer Plymer, JiuJiang, JiangXi, China) and polydimethylsiloxane (PDMS; Yuil Tech, Daegu, South Korea) were selected as candidate materials for the head spring.[8,9] Sheets of both materials (2-mm thick) were cut via cylindrical metal punch into disks (11-mm diameter) for pressing (1200 psi, 5 min, room temperature) in metal molds.

Design of novel aneurysm clip

A. Single biomaterial clips: Titanium, PEEK, and zirconia

In devising a novel aneurysm clip, samples were first attempted by changing the physical properties of conventional clip material. A titanium cylinder bundle with lamellar structure served to recreate existing clip design, varying the number of rods used (Figure 1).

Various clips were also configured using polyetherether ketone (PEEK), a type of polymer. Zirconia clips without spring parts were fabricated as well (Figure 2).

B. Hybrid clips

Precision design of our prototypic ZC was achieved through computer-aided solid-modeling design software (SolidWorks Corp, Waltham, MA, USA), mimicking the commercially available 8.3-mm titanium Yasargil clip (YC) (FT750T; Aesculap AG, [B Braun Group], Tuttlingen, Germany). Total length of the ZC was 19.4 mm (same as YC), and its width was 1.5 mm (thicker than YC by 0.5 mm). The ZC has two parts: blade (length, 9 mm) and spring (head size, 6 mm). Head size of the spring part was designed for secure intraoperative placement. To prevent straying of the polymer spring, the inner blade legs were serrated, and four spring configurations were devised: hollow cube, crescent, S shape, and I shape (Figure 3).

The YC (FT752T: curved, 8.3 mm long) and Sugita clip (SC) (07-940-02: straight, 10 mm long]; Mizuho Medical Co, Tokyo, Japan) served as comparator devices. The YC and SC are made of titanium (Ti-6Al-4V) and cobalt-chrome (Co-Cr-Ni-Mo-Fe) alloy, respectively.[10-13]

Closing force magnitude and opening width

The aneurysm clip was assembled with various polymer springs for testing of closing force. Once design was complete, clips with an array of ceramic blades were machined using a high-precision laser system (VLS4.60; Universal Laser Systems Inc, Scottsdale, AZ, USA) for cutting of nonmetallic substrates. Eight differently shaped polyurethane or PDMS springs were fabricated from polymer sheets pressed (1200 psi, 5

min, room temperature) in metal molds.

Closing force and open-blade width were gauged using a universal testing machine (Model 3343; Instron [ITW], Norwood, MA, USA) under fixed loading rate (1 mm/min). The testing protocol was set to measure closing force continuously at blade gap distances from 0.5-2.0 mm. Closing force exerted by each clip was expressed in Newtons (N), measuring spring force at 1 mm from blade tips. Closing forces of the final spring design (through process of exclusion) were compared with YC and SC closures at 1 mm, 3 mm, and 8 mm from blade tips and at 1-mm blade gap.

MR compatibility assessment

All MR imaging entailed use of a 3T MR scanner (Magnetom Trio TIM; Siemens Medical Solutions, Erlangen, Germany) equipped with a 12-channel head coil. In vitro MR imaging of titanium clips included time-of-flight (TOF) MRA of phantoms in 3D multi-slab gradient-echo sequence (TR/TE, 23/4.2 ms; flip angle, 10° ; 4 slabs, each with 14 partitions; FOV, 146 × 180 mm; matrix, 512 × 208; slice thickness, 0.8 mm), using generalized autocalibrating partially parallel acquisition (GRAPPA).

To compare the susceptibility artifact volumes of ZC, YC, and SC in MR images, both turbo spin-echo T2-weighted imaging (T2WI: TR/TE, 6000/87 ms; flip angle, 120° ; FOV, 96 × 120 mm; matrix, 320 × 230; slice thickness, 1.5 mm; intersection gap, 0.3 mm) and gradient-echo TOF MRA (TR/TE, 27/4.9 ms; flip angle, 10° ; FOV, 120 × 120 mm; matrix, 512 × 192; slice thickness, 1.0 mm) with GRAPPA were applied, generating two separate datasets in axial and coronal planes.

In vivo MRA of the canine aneurysm model was performed with turbo

spin-echo T2WI, gradient-echo TOF MRA, and contrast-enhanced (CE) MRA with gadoterate meglumine (Dotarem; Guerbet, Aulnay-sous-Bois, France) (0.1 mmol per kilogram of body weight) as following parameters: T2WI (TR/TE: 6190/91 ms, flip angle: 131° , FOV: 163 x 180 mm, a matrix of 640 × 290, slice thickness: 5.0 mm), TOF MRA (TR/TE: 23/4.2 ms, flip angle: 18° , FOV: 146 × 180 mm, a matrix of 512 × 208, section thickness: 0.6 mm, GRAPPA), and CE MRA (TR/TE: 3/1.2 ms, flip angle: 26° , FOV: 200 × 320 mm, a matrix of 448 × 168, section thickness: 0.7 mm). These data were reconstructed in coronal plane to evaluate artefactual clip volumes in canine neck vessels.

MR compatibilities of raw materials in disk shape and clips in in vitro conditions (a 1.5 wt% agarose gel in distilled water phantom) were assessed to simulate tissue interaction. Imaging planes for axial, coronal, and sagittal scans were oriented in perpendicular and parallel positions, along short and long axes of specimens. MR images and artefactual areas and volumes of raw materials and clips were captured and quantified using a domestic picture archiving and communications system (PACS; INFINITT Co, Seoul, South Korea).

Side-wall aneurysm model (canine venous pouch)

All procedures were approved by the local Institutional Animal Care and Use Committee and were conducted according to international guidelines. A male Mongrel, aged 6.5 months and weighing 31 kg, was used in this study. The canine was acclimated for 2 weeks before surgery, conducting procedures in sterile conditions under general anesthesia. The latter was induced intramuscularly, using zoletil (5 mg/kg) and xylazine (2 mg/kg). The canine was then intubated, and

intravenous 0.9% normal saline (5 mL/kg/hr) was administered via leg vein. Anesthesia was maintained using isoflurane (2-4%, 2-3 L/min) and oxygen/nitrogen (3 L/min). Vital parameters, such as arterial blood pressure, heart rate, and carbon dioxide levels, were continuously recorded. Expired carbon dioxide levels were maintained at 35-40 mm Hg.

A 10-cm skin incision was made at each side of anterolateral neck, with the animal in supine position. A segment (~6.0 cm) of external jugular vein was harvested, preparing four venous pouches of 1-cm length and storing them in heparinized saline. Both common carotid arteries (CCAs) were subsequently exposed. Upon clamping proximal and distal CCA, two 1-cm linear arteriotomies of each CCA were performed (~4 mm apart), using 8-0 prolene suture for anastomosis (end to side) of one venous pouch per arteriotomy. Thus, a bilateral model of aneurysms was generated, constructing dual venous pouches on each CCA. The two sites on each side were adequately separated and were staggered (~1 cm) right to left to minimize susceptibility artifact of clips in MR images. As a matter of convention, aneurysms and clips were assigned as follows: right upper CCA (An 1), SC; right lower CCA (An 2), unclipped control; left upper CCA (An 3), ZC; and left lower CCA (An 4), YC.

To confirm patency of parent arteries and status of model lesions, a system we previously developed (endoscopic indocyanine green [ICG] angiography) was applied.[14] Briefly, ICG is injected via leg vein as a bolus dose (0.3 mg/kg), using a 10-mm straight endoscope capable of simultaneous visible color and ICG fluorescent imaging to monitor outcomes before and after clipping. This method is noninvasive and easy to use, unlike conventional angiography under fluoroscopy via

femoral artery.

After creating the model aneurysms and checking the efficacy of clipping, the wounds were closed, and the canine was cared for by a veterinarian. Three days postoperatively, MR was done to confirm and compare MR susceptibility artifacts of YC, SC, and ZC. Seven weeks after surgery, the dog was euthanized to harvest the model aneurysms for comparative gross and histologic examinations. The specimens were fixed in paraformaldehyde and processed routinely for histologic sections and staining.

Results

MR compatibility of raw materials

Four discs made of raw materials for potential use in clip body (TiO_2 and ZrO_2) and head spring (polyurethane and PDMS) were examined (Figure 4). In TOF MR images, artefactual volumes of ZrO_2 in both axial and coronal planes were closer to actual volumes than those of TiO_2 (1.1- vs 1.5-fold greater), whereas polyurethane and PDMS showed little disparity between actual and MR-based volumes (Table 1). The MR artifact ratio of every disc was similar in all directions.

Closing force and opening width of clips

None of the PEEK clips could overcome their polymeric limitations (compared with metals or ceramics), and they were not sufficiently strong to share the mechanical properties of a conventional YC (Figure 5 & 6).

Various designs of ZC without spring parts had been attempted (Figure 2) to impart mechanical compatibility comparable to the YC. However, the clip head in these designs was cumbersome and impractical.

In ZC closing force determinations, with four variably shaped head springs of either polyurethane or PDMS (eight permutations), polyurethane far exceeded PDMS in like designs. Closing forces of three head spring shapes (hollow cube, I shape, and S shape) in PDMS and the crescent-shaped head spring in polyurethane are displayed in Figure 7. Closing forces were excessive for the three other head spring shapes in polyurethane, culminating in breakage upon opening; and the crescent-shaped head spring in PDMS displayed lower closing force by

comparison and its closing force could not show in graph. Maximal open-blade widths of the various body/head spring combinations were also tested (Table 2). Ultimately, closing force and open-blade width of the crescent-shaped polyurethane head spring proved optimal for ZC.

Closing forces of YC, SC, and ZC were measured in various scenarios (Figure 8). Force was first applied at 1 mm from blade tip, rising continuously as clips opened, regardless of clip type. Values for each clip were similar, until open-blade width reached ~1.15 mm. Thereafter, the closing force of ZC rose abruptly. Closing force was highest for ZC, followed by YC and then SC. Respective closing forces (N) at 1 mm from blade tip at opening widths of 0.5, 1.0, 1.5, and 2.0 mm were 1.54, 2.09, 2.24, and 2.35 for YC; 1.50, 1.85, 2.06, and 2.20 for SC; and 1.48, 2.05, 2.76, and 3.44 for ZC.

The closing forces of all clips became higher as distance from blade tip increased. All values at ~3 mm from the tip were similar, but progressively increased (ZC >YC >SC) with increasing distance from blade tip. Respective closing forces (N) at 1, 3, and 8 mm from blade tip were 2.09, 2.30, and 3.77 for YC; 1.85, 2.33, and 3.04 for SC; and 2.05, 2.20, and 4.60 for ZC.

MR compatibility in vitro and in vivo

YC was MR-tested in various planes (Figure 9). Titanium clips made of lamellar cylinder bundles were similarly tested (Figure 10), but these particular structural changes resulted in scant MR susceptibility reduction.

Weights and actual volumes of each clip were measured as 0.20 g and 0.045 cm^3 for YC; 0.16 and 0.036 for SC; and 0.53 and 0.088 for ZC

body. Compared with actual volumes of each clip, respective artefactual volumes of YC, SC, and ZC in agarose gel phantoms were 26.9-, 29.7-, and 1.7-fold greater in gradient-echo TOF MR imaging and in spin-echo T2WI were 26.0-, 33.7-, and 2.0-fold greater than actual volumes. Clip volumes in various scenarios are summarized in Table 3 and Figure 11.

Four aneurysms (An 1, SC; An 2, control; An 3, ZC; and An 4, YC) in a canine venous pouch aneurysm model are shown before and after clipping in Figure 12. Using an endoscopic ICG angiography system, patency of both carotid arteries and aneurysms was ensured before clipping, and flow to clipped aneurysms (An 1, 3, and 4) from parent arteries was proven completely obstructed after intentional clipping to remain residual sac. In our in vivo aneurysm model, artefactual volumes of YC, SC, and ZC by TOF MR imaging were 21.4-, 29.4-, and 2.6-fold greater than corresponding actual volumes. Measured volumes and representative photos are provided in Table 3 and Figure 12. At 7 weeks postoperatively, the experimental canine was healthy, and all clips were well positioned at autopsy, with no evidence of slippage or adjacent tissue abnormalities (Figure 13). On histologic examination, normal healing was evident in both An 1 and An 2. However, severe inflammation was identified in An 3 and in An 4, making it difficult to compare tissue reactions by nature of clip (commercial vs ZC).

Discussion

In patients with clipped aneurysms, MR brain imaging may be variably limited by artifacts. Clipping and coil embolization procedures may indeed constrain the utility of either CTA or MR imaging in postoperative evaluations of cerebral aneurysms. However, MR imaging is an increasing need for a variety of reasons. In patients with clipped aneurysms, technologic advances in MR imaging are imperative to reduce metal artifacts, and there is a growing demand for clips of new materials.

This study was subsequently aimed at developing a MR-compatible clip with mechanical properties comparable to conventional clips. We were also intent on verifying its clinical applicability through *in vitro* and *in vivo* testing. Mechanical and MR compatibility testing was applied to all of the various clips made from an array of biocompatible materials, including conventional biosubstances.

Slice encoding and view-angle tilting have been used to reduce metal artifact in MRI studies of orthopedic implants.[7] Although the diminutive sizes of aneurysm clips may defy such efforts, the higher resolution conferred to 3-dimensional CTA through multislice scanners currently enables better postoperative delineation of clip placement. Nevertheless, not only are there issues in terms of radiation exposure and contrast use, but the metal artifacts encountered after applying multiple clips or cobalt-alloy clips are problematic. 2 The standard modality for evaluating cerebral aneurysms after clipping or coil embolization, which is DSA, is invasive and also poses radiation/contrast hazards. However, by reducing susceptibility artifact in MRI studies, the inherent benefits

of this particular modality (ie, noninvasiveness, no radiation danger or need of contrast) may ultimately be realized in this setting.

Titanium clips incorporating existing materials for structural modifications (prior to the introduction of new resources) did not significantly reduce MR susceptibility. Thus, we concentrated on polymeric or ceramic biomaterials, exhibiting lower MR susceptibility than titanium, for clip fabrication. Among the possibilities, PEEK demonstrated chemical, thermal, and radiation stability and has been used for a variety of biologic implants.[15] Unfortunately, in strength-testing against metal and ceramic alternatives, it proved ill-suited as clip material.

Compared with other biomaterials, ceramics result in considerably less MR artifact and are viewed as the most suitable substrate for clips, despite lower retention force or less flexibility than metallic devices. Among its ceramic competitors, zirconia is reported to produce the least MR artifact;[4] *in vitro* and *in vivo* experiments of zirconia in orthopedics and dentistry demonstrated tissue compatibility and stability.[16,17] And in this experimental comparison of a zirconia prototype with other commercially available clips, zirconia did show superior MR compatibility. Unfortunately, the use of metal head springs in prior ceramic clip designs failed to eliminate MR susceptibility artifact, which is why we scrutinized head spring constructs with equal intensity. Polyurethane and PDMS were tested as candidate materials for the head spring. Four different designs of clips were made from each material and a clip of a crescent shape made of polyurethane was selected by comparing the closing force and the opening width.

Reflecting mechanical properties, the respective values for Young's modulus (GPa) and fracture toughness (MPa $m^{1/2}$) were 114-120 and

65-90 in titanium clips, 220-230 and 100 in cobalt-chrome alloy clips, and 206 and 7.4 in the ZC.[18] Thus, the ZC body proved more elastic but lower in fracture toughness than commercial clips.[16] A 1.5-mm width (0.5 mm thicker than YC) was selected in this study, knowing that zirconia is more brittle than titanium and cobalt-chrome alloys.[19,20,21]

Mechanical shortfalls notwithstanding, the ZC showed no problems when applied to our animal model for *in vivo* testing. The narrow open-blade width is clearly a limiting factor in practical application that may yet be resolved through modified head design. Certainly, the heftier body fabrication used to overcome mechanical weakness was not an impediment. *In vitro* and *in vitro* MR artifacts were significantly reduced by comparison. In MR images obtained after clipping, performance of the ZC was vastly superior to two other commercial clips, presumably a result of novel body and head spring fabrication. MR images of an aneurysm that was intentionally incompletely clipped by ZC showed the residual sac and parent artery most clearly.

There were certainly some acknowledged limitations to this experimental study. Although blood flow was obstructed after clipping in our canine model, the ZC blade was not tight, leaving a between-blade gap. This was a technical problem (ie, manufacturing defect). Open-blade width of the ZC was troublesome as well and should be addressed. Overall, this prototype was somewhat heavy, unstable, and weak, with room for improvement but lacking a competitive advantage over commercial clips at present. Experimentation with other spring shapes and a design implementation that can reduce blade width while maintaining blade strength are needed. Long-term durability of the ZC was not explored at this time, nor were other tactical scenarios

(incomplete clipping, clipped and coiled aneurysms, or multiple clip application); and MR imaging by region of interest is another future pursuit. Ultimately, commercialization of zirconia clips with crescent-shaped head springs would require substantial advances in product design and manufacturing. Although the biocompatibility of zirconia is already established,[16,17] the tissue reactions to commercial clips and to ZC have been difficult to compare in the histologic preparations undertaken.

Conclusion

Zirconia as a raw material for clip fabrication produces superior MR compatibility. *In vitro* and *in vivo* experimentation confirmed the least susceptibility artifact for the ZC prototype (vs commercially available aneurysm clips), with satisfactory closing forces. However, its modest open-blade width is a weak point. Further experiments under various conditions are needed for design refinements, durability testing, and eventual human application.

References

1. Lin N, Cahill KS, Frerichs KU, Friedlander RM, Claus EB. Treatment of ruptured and unruptured cerebral aneurysms in the USA: a paradigm shift. J Neurointerv Surg. 2012 May;4(3):182-189.

2. Reichert M, Ai T, Morelli JN, Nittka M, Attenberger U, Runge VM. Metal artefact reduction in MRI at both 1.5 and 3.0 T using slice encoding for metal artefact correction and view angle tilting. Br J Radiol. 2015 Apr;88(1048):20140601-20140611.

3. Wichmann W, Von Ammon K, Fink U, Weik T, Yasargil GM. Aneurysm clips made of titanium: magnetic characteristics and artifacts in MR. AJNR Am J Neuroradiol. 1997 May;18(5):939-944.

4. Matsuura H, Inoue T, Konno H, Sasaki M, Ogasawara K, Ogawa A. Quantification of susceptibility artifacts produced on high-field magnetic resonance images by various biomaterials used for neurosurgical implants. Technical note. J Neurosurg. 2002 Dec;97(6):1472-1475.

5. Sagara Y, Kiyosue H, Hori Y, Sainoo M, Nagatomi H, Mori H. Limitations of three-dimensional reconstructed computerized tomography angiography after clip placement for intracranial aneurysms. J Neurosurg. 2005 Oct;103(4):656-661.

6. Cho WS, Kim SS, Lee SJ, Kim SH. The effectiveness of 3T time-of-flight magnetic resonance angiography for follow-up evaluations

after the stent-assisted coil embolization of cerebral aneurysms. Acta Radiol. 2014 Jun;55(5):604-613.

7. Cho YD, Kim KM, Sohn CH, Kang HS, Kim JE, Han MH. Time-of-flight magnetic resonance angiography for follow-up of coil embolization with enterprise stent for intracranial aneurysm: usefulness of source images. Korean J Radiol. 2014 Jan-Feb;15(1):161-168

8. Shkol' nik SI, Shimanskii VM. Mechanical properties of polyurethane elastomers. Fisiko-Khimicheskaya Mekhanika Materialov. 1966;2(5):538-542.

9. Mata A, Fleischman AJ, Roy S. Characterization of polydimethylsiloxane (PDMS) properties for biomedical micro/nanosystems. Biomed Microdevices. 2005 Dec;7(4):281-293.

10. Niinomi M. Mechanical properties of biomedical titanium alloys. Materials Science and Engineering: A. 1998 Mar;243(1-2):231-236.

11. Hofmann DC, Suh JY, Wiest A, Lind ML, Demetriou MD, Johnson WL. Development of tough, low-density titanium-based bulk metallic glass matrix composites with tensile ductility. Proc Natl Acad Sci USA. 2008 Dec 23;105(51):20136-201340.

12.https://www.aesculapusa.com/assets/base/doc/instructions/aic/neurosurgery/Yasargil_Permanent_Aneurysm_Clips_SOP-AIC-5000566_(TA011251-US).pdf

13.http://www.mizuho.com/wp-content/uploads/2014/05/Elgiloy-Brochure-Apr-2014.pdf

14. Cho WS, Kim JE, Kim SH, Kim HC, Kang U, Lee DS. Endoscopic Fluorescence Angiography with Indocyanine Green: A Preclinical Study in the Swine. J Korean Neurosurg Soc. 2015 Dec;58(6):513-517.

15. Kurtz SM (Editor). PEEK Biomaterials Handbook. Elsevier. 2011

16. Manicone PF, Iommetti PR, Raffaelli L. An overview of zirconia ceramics: basic properties and clinical applications. Journal of Dentistry 2007;35(11):819-826.

17. Ichikawa Y, Akagawa Y, Nikai H, & Tsuru H. Tissue compatibility and stability of a new zirconia ceramic in vivo. Journal of Prosthetic Dentistry 1992;68(2):322-326.

18. Ogawa M, Tohma Y, Ohgushi H, Tarakura Y, Tanaka Y. Early Fixation of Cobalt-Chromium Based Alloy Surgical Implants to Bone Using a Tissue-engineering Approach. Int J Mol Sci 2012;13(5):5528-5541

19. Gogotsi G, Mudrik S, Galenko V. Evaluation of fracture resistance of ceramics: Edge fracture tests. Ceramics Internationals. 2007 Apr;33(3):315-320.

20. Palmeira AA, Bondioli MJ, Strecker K, dos Santos C. Densification and grain growth of nano- and micro-sized Y-TZP powders. Ceramics Internationals. 2016 Feb;42(2):2662-2669.

21. Chevalier J and Gremillard L. Zirconia as a biomaterial. Comprehensive Biomaterials. Paul Ducheyne (Editor in Chief), Vol 1. Metallic, Ceramic and Polumeric Biomaterials. Elsevier. pp95-108. 2011

국문초록

자기장 내 영상 왜곡을 최소화하기 위한 새로운 재질의 뇌동맥류 결찰술용 클립 개발연구

서울대학교 대학원
의학과 신경외과학 전공
손 영 제

목적: 뇌동맥류 클립 결찰술 이후에 추적영상으로서 자기공명영상은 클립으로 인한 영상 왜곡이 심하여 적합하지 않다. 비침습적이고 방사선 피폭이 없는 자기공명영상을 이용한 영상 추적을 위해 영상 왜곡을 최소화할 수 있는 클립을 개발하고자 한다.

방법: 인체에 적합하고, 자기공명영상에 적합하여 영상 왜곡을 최소화하며 뇌동맥류 치료에 충분한 기계적 특성을 가질 수 있는 금속, 세라믹 및 폴리머 재료 중, 지르코니아 (몸체)와 폴리우레탄 (스프링)으로 클립을 제작하였다. 현재 사용되고 있는 클립 (Yasargil 클립, YC과 Sugita 클립, SC)과 지르코니아 클립 (ZC)의 자기공명 영상 왜곡의 정도와 물리적 특성을 생체외 및 동맥류 실험동물 모델에서 비교를 하였다.

결과: 블레이드 끝으로부터 1mm 및 8mm 거리에서 측정한 각각의 폐쇄

력 (N) 값은 YC에서 2.09 및 3.77, SC에서 1.85 및 3.04, ZC에서 2.05 및 4.60이었다. 최대 개방 폭 (mm)은 각각 YC, SC 및 ZC에서 6.8, 9.0 및 3.0이었다. YC 및 ZC의 체외 자기공명영상 부피는 해당 실제보다 26.0 배 및 1.9 배 더 컸다. YC, SC 및 ZC의 생체 내에서의 자기공명영상 부피는 실제보다 21.4 배, 29.4 배 및 2.6 배 더 컸다.

결론: 현재 사용 중인 두 개의 클립과 비교할 때 프로토 타입의 지르코니아 클립은 닫는 힘이 뇌동맥류 폐색에 충분한 폐쇄력이 있으면서 자기공명영상 감수성이 제일 적었다. 그러나 좁은 개방 폭은 약점이었다. 인체 적용을 위해 클립의 설계 개선 및 내구성 시험을 위한 추가 실험이 필요하다.

.....

주요어 : 자기공명영상 적합성, 뇌동맥류, 클립, 지르코니아, 영상 왜곡
학 번 : 2004-30621

Figures

Figure 1. Titanium clips made from lamellar cylinder bundles

Figure 2. Design of zirconia clips, devoid of spring parts

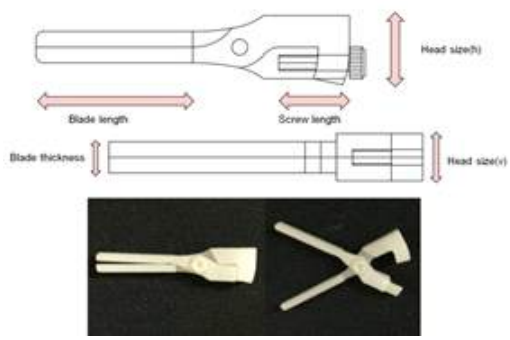

Figure 3. Design of novel aneurysm clip, including clip body (A and B) and head spring (C: hollow cube; D: crescent; E: S shape; F: I shape).

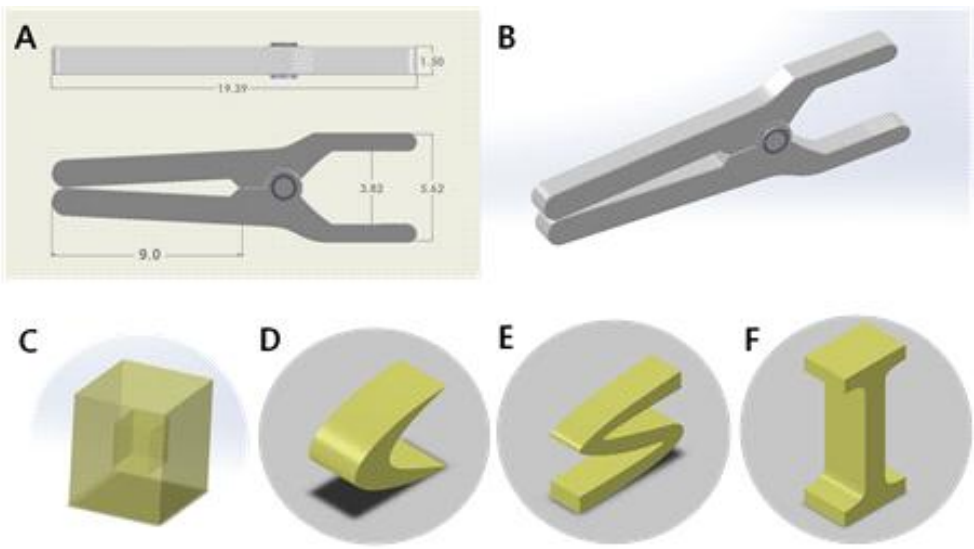

Figure 4. MR susceptibility artifact of prospective raw materials in novel clip: (A) TiO2 and (B) ZrO2 for clip body; (C) polyurethane and (D) PDMS for head spring (actual digital photographs and TOF MR views).

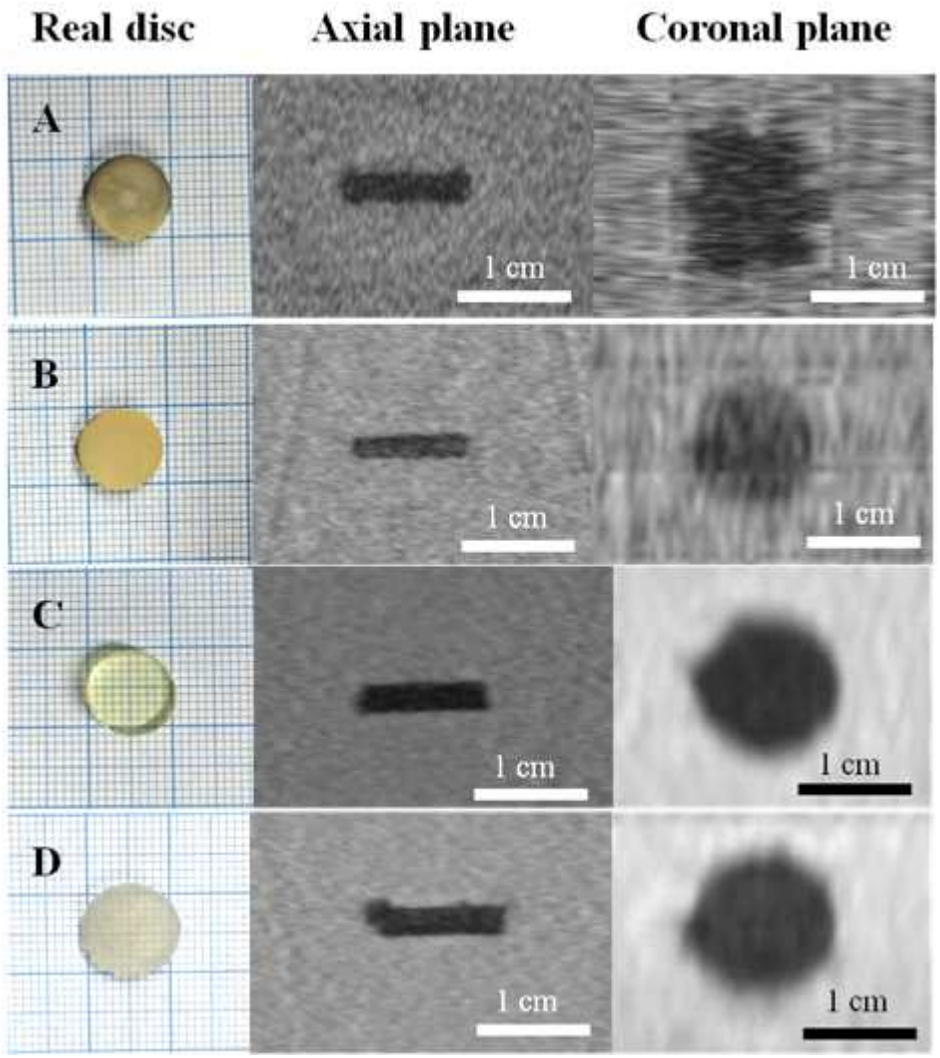

Figure 5. Mechanical properties of PEEK clip, without box or bar lock.

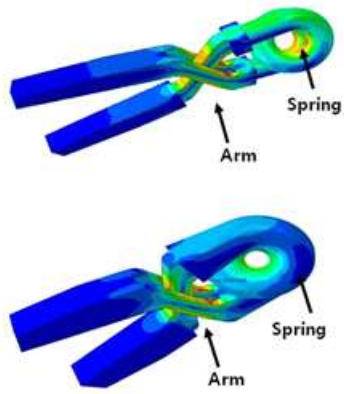

Opening	1mm	3mm	5mm
Stress_spring (MPa)	24.3	73.7	124.3
Stress_arm (MPa)	26.0	78.1	130.2
Strain_spring (%)	0.14	0.42	0.71
Strain_arm (%)	0.25	0.75	1.26
Closing Force (N)	0.32	0.98	1.68

Opening	1mm	3mm	5mm
Stress_spring (MPa)	26.9	92.4	159.5
Stress_arm (MPa)	45.5	142.6	242.2
Strain_spring (%)	0.17	0.62	1.08
Strain_arm (%)	0.46	1.44	2.50
Closing Force (N)	1.79	5.68	9.89

Figure 6. Mechanical properties of PEEK clip, with single box lock.

1. Optimized C shape spring

Opening	1mm	3mm	5mm
Stress (MPa)	46.0	125.2	209.1
Strain (%)	0.47	1.40	2.34
Closing Force (N)	1.05	3.13	5.22

2. Half spring

Opening	1mm	3mm	5mm
Stress (MPa)	63.1	191.2	324.6
Strain (%)	0.47	1.47	2.54
Closing Force (N)	2.21	6.77	11.74

3. 1.5 coil spring

Opening	1mm	3mm	5mm
Stress (MPa)	34.7	105.5	179.3
Strain (%)	0.27	0.83	1.41
Closing Force (N)	2.66	8.10	13.96

Figure 7. Closing force measurement: At the head of zirconia clip (arrow in A), four spring designs in both polyurethane and PDMS (total of eight) were subjected to closing force measurement (B). Three of the polyurethane spring designs inflicted breakage upon opening, and the crescent-shaped PDMS variant registered lower than the polyurethane counterpart. Residual closing forces (C) are charted as 1, hollow cube PDMS spring; 2: crescent-shaped polyurethane spring; 3, I-shaped PDMS spring; and 4, S-shapes PDMS spring.

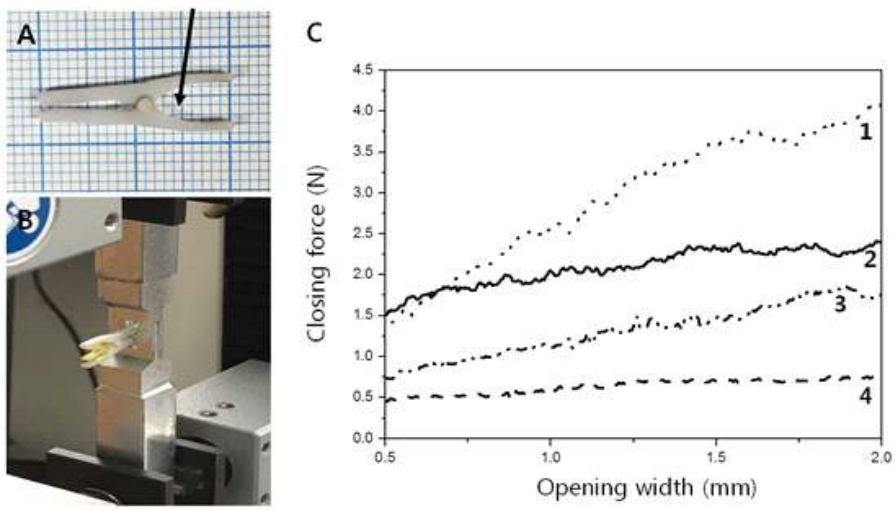

Figure 8. Closing force at 1 mm from blade tip plotted by (A) open-blade width and (B) distance from blade tip for Zirconia (line 1), Sugita (line 2), and Yasargil (line 3) clips.

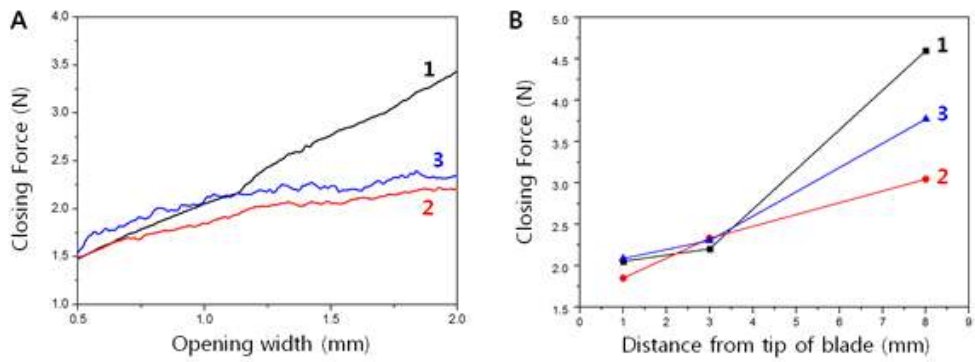

Figure 9. *In vitro* MR test of YC in multiple planes

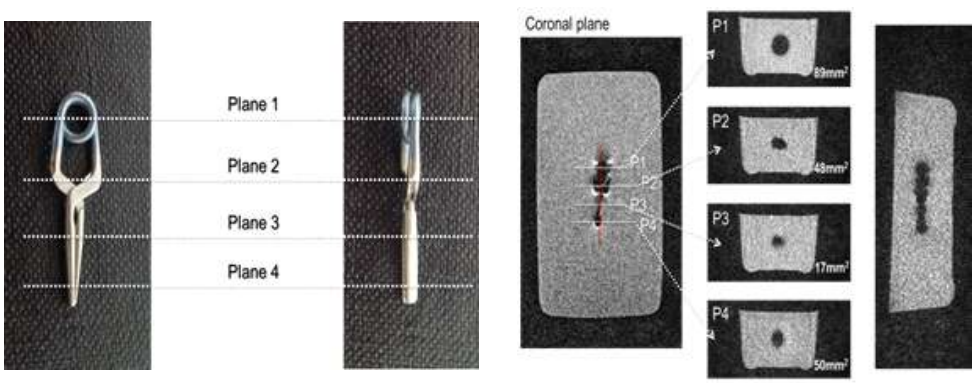

Figure 10. Comparison of MR image on the same plane (YC and Titanium clips using a cylinder bundle consisting of a lamellar structure)

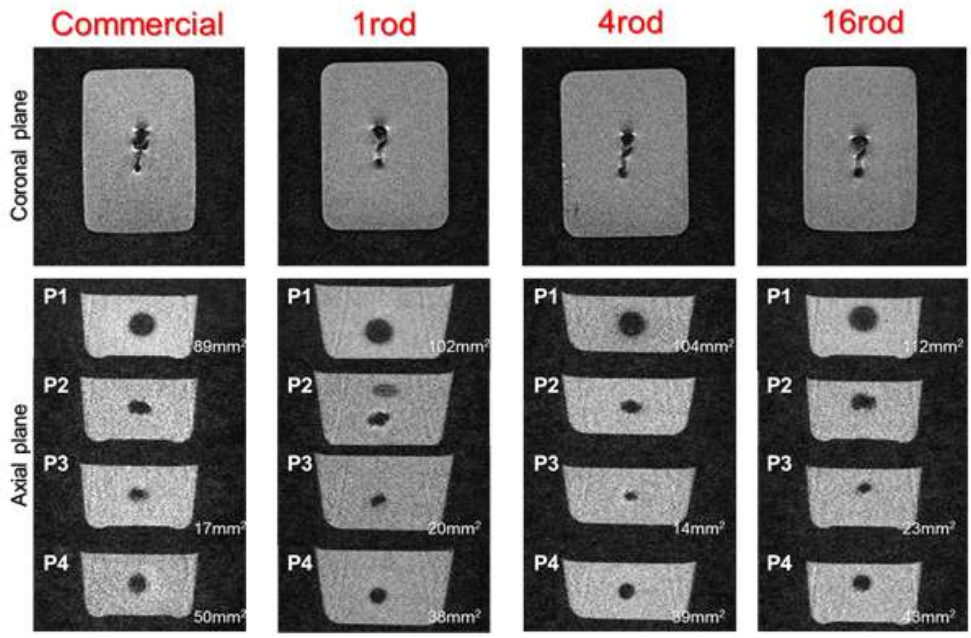

Figure 11. Actual clips (left) and MR imaging of (A) Yasargil, (B) Sugita, and (C) zirconia clips in agarose phantoms (not represented by 1:1 magnification).

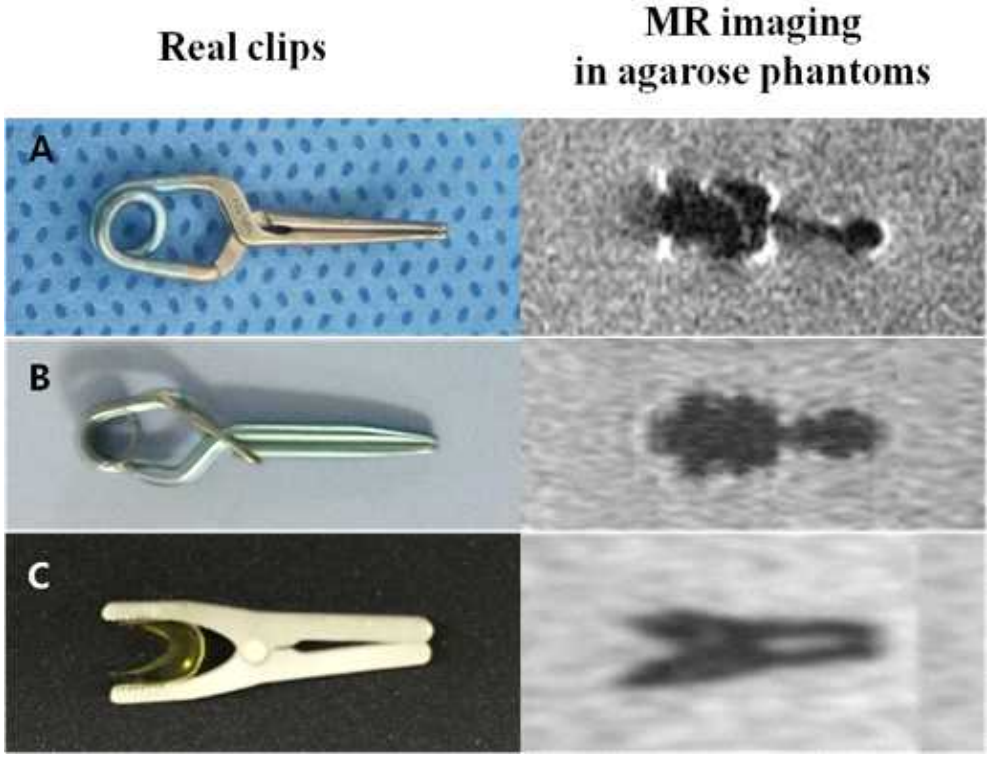

Figure 12. Canine aneurysm (An) model of common carotid artery (CCA): (A) An 1 and An 2 of right CCA, and (B) An 3 and An 4 of left CCA were clipped using (C) Sugita (An1), (D) zirconia (An3), and (E) Yasargil (An4) devices, An 2 serving as unclipped control; (F–H) residual necks of An 1, An 3, and An 4 in endoscopic fluorescence images; and (I and J) all clips intact at autopsy, without slippage.

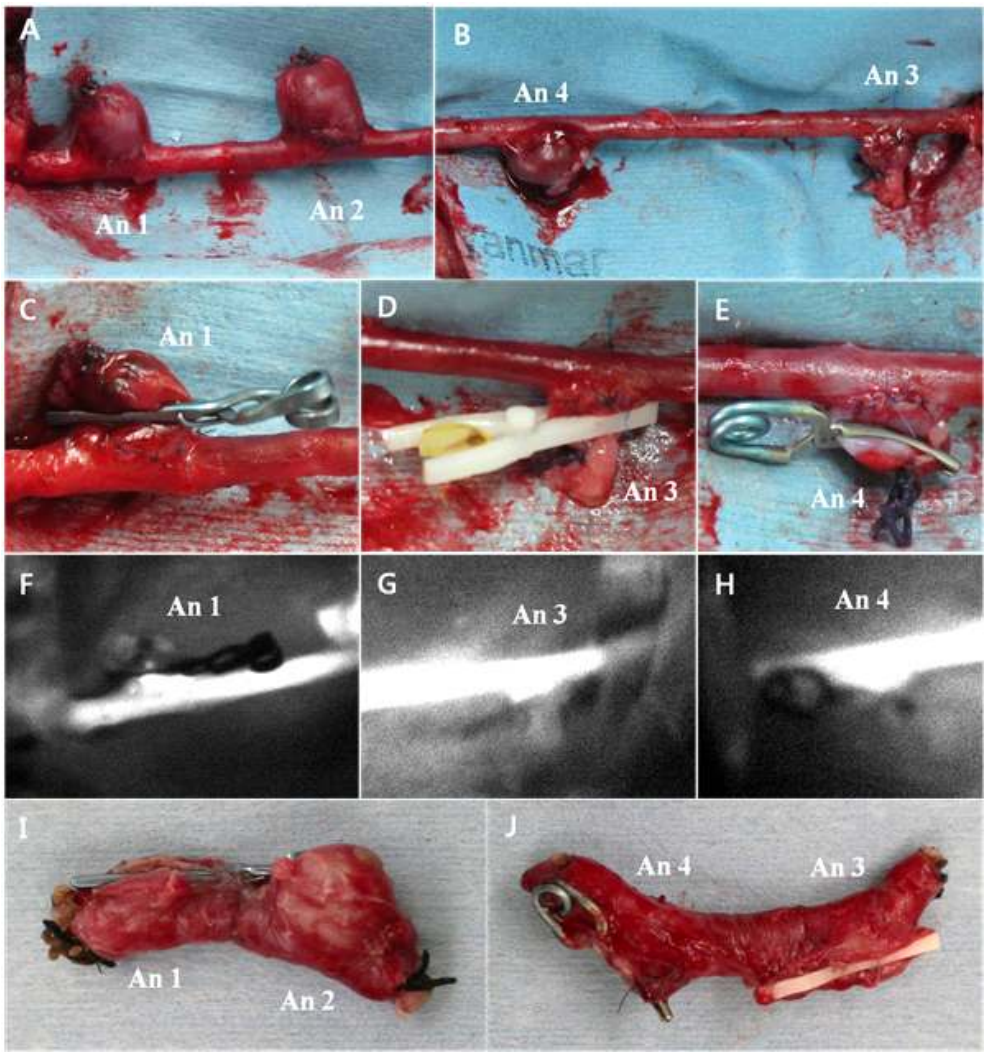

Figure 13. *In vivo* MR imaging of clips in canine aneurysm model: Maximal intensity projection images of (A) right and (B) left common carotid arteries, demonstrating residual necks or sacs of aneurysms (An) 1-4; and coronal views reconstructed from TOF source images, showing (C, bold arrow) Sugita, (D, dotted arrow) zirconia, and (E, long arrow) Yasargil clips.

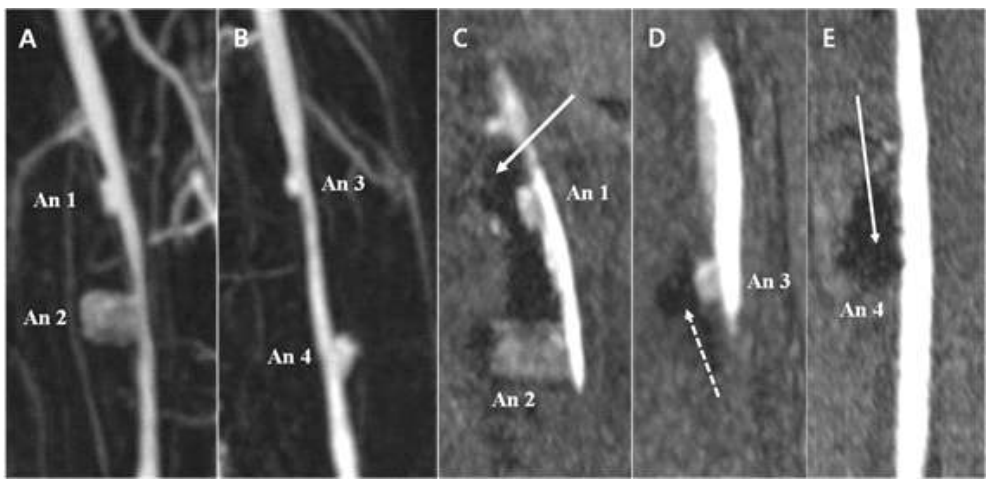

Tables

Table 1. MR susceptibility artifact: actual vs artefactual raw material sizes

Raw materials	Plane	Actual size (A)	Artefactual size in MR (B)	B/A
TiO_2disc	Coronal	0.862	1.292	1.5
	Axial	0.228	0.348	1.5
ZrO_2disc	Coronal	0.869	0.990	1.1
	Axial	0.210	0.240	1.1
Polyurethane disc	Coronal	0.950	0.891	0.9
	Axial	0.220	0.213	1.0
PDMS disc	Coronal	0.950	0.956	1.0
	Axial	0.220	0.225	1.0

Table 2. Maximum open-blade width according to clip specifications

Clip materials/head spring shape	Maximum open-blade width (mm)
YC (FT752T)	6.8
SC (07-940-02)	9.0
ZC	
Without head spring	4.35
Hollow cube shape, PDMS	1.52
Crescent shape, polyurethane	3.02
S shape, PDMS	2.43
I shape, PDMS	3.15

YC: Yasargil clip, SC: Sugita clip, ZC: Zirconia clip

Table 3. Clip volumes in various scenarios

	Yasargil Clip	**Sugita Clip**	**Zirconium Clip**
Actual volume (vol.)	0.045 (1)	0.036 (1)	0.088 (1)
Artefactual vol. in agarose gel			
TOF MR imaging	1.211 (26.9)	1.069 (29.7)	0.146 (1.7)
T2W MR imaging	1.170 (26.0)	1.217 (33.7)	0.179 (2.0)
Artefactual vol. in canine model	0.965 (21.4)	1.060 (29.4)	0.228 (2.6)

Clip volumes expressed as cm^3, with artefactual volume ÷ actual volume in parentheses

TOF: time-of-flight, MR: magnetic resonance, T2W: T2-weighted